# Surfing surface gravity waves

## Nick E. Pizzo†

Scripps Institution of Oceanography, University of California, San Diego, La Jolla,
CA 92093-0213, USA

A simple criterion for water particles to surf an underlying surface gravity wave is presented. It is found that particles travelling near the phase speed of the wave, in a geometrically confined region on the forward face of the crest, increase in speed. The criterion is derived using the equation of John (*Commun. Pure Appl. Maths*, vol. 6, 1953, pp. 497–503) for the motion of a zero-stress free surface under the action of gravity. As an example, a breaking water wave is theoretically and numerically examined. Implications for upper-ocean processes, for both shallow- and deep-water waves, are discussed.

**Key words:** air/sea interactions, surface gravity waves, wave breaking

## 1. Introduction

This study reports on a theoretical criterion for particles to surf water waves. Here, a particle travelling near the phase velocity of the underlying wave that experiences an increase in its horizontal velocity due to the wave is said to surf. The theory is based on an analysis of the John equation (John 1953) for zero-stress free-surface flows under the action of gravity. Employing this equation, it is shown that particles in the region of the forward face of the crest of a very steep or breaking wave, travelling at speeds near the phase velocity of the underlying wave, increase in speed. This is the main result of this paper.

As any experienced surfer knows, the ideal location to be on a wave is near the forward face of the crest of an unbroken wave approaching breaking. This is commonly referred to as the 'curl'. Staying in the curl maximizes distance travelled, which is correlated with the ride enjoyment. A similar phenomenon occurs when white water from a breaking wave rides the underlying wave, which is an important process in both shallow and deep-water upper-ocean dynamics.

Shallow-water breaking waves transport mass, generate currents and mix the surf zone (Inman, Tait & Nordstrom 1971; Peregrine 1983; Battjes 1988). Wave breaking in the surf zone radically alters along-shore currents, versus the traditional model of gradients in the radiation stress (Longuet-Higgins & Stewart 1964; Feddersen *et al.* 2016). Mixing is crucial for regulating the thermodynamics (Sinnett & Feddersen 2014) and chemistry (Bresnahan *et al.* 2016) in the near-shore region, while currents transport pollutants along the coastline (Feddersen 2007; Clark, Feddersen & Guza

† Email address for correspondence: npizzo@ucsd.edu

2010). A better understanding of breaking is important for characterizing near-shore processes.

The Lagrangian drift, or mass transport, of deep-water surface waves is an important feature of upper-ocean dynamics (Phillips 1977). Traditionally, the drift is associated with permanent progressive waves and for linear waves this is known as Stokes drift. Stokes drift is believed to be essential for generating Langmuir circulations (Craik & Leibovich 1976; Leibovich 1983; McWilliams, Restrepo & Lane 2004), as well as transporting mass, which might strongly modulate global ocean circulation (McWilliams & Restrepo 1999). However, Stokes drift is very difficult to measure in the ocean and its form for realistic sea states is still an active area of research (Smith 2006).

Alternatively, wave breaking, which is intermittent in space and time, transports mass and generates ocean currents (Rapp & Melville 1990; Melville, Veron & White 2002). Direct numerical simulations (Sullivan, McWilliams & Melville 2004) and large eddy simulations (Sullivan, McWilliams & Melville 2007) show that wave breaking, using a simple body force model for the effects of breaking on the mean flow, is an important component of the dynamics of the upper ocean. This motivated a closer examination of the integral properties of the breaking induced flow (Pizzo & Melville 2013; Pizzo, Melville & Deike 2016) in the context of impulsive forces and vortex dynamics.

Similarly, very recently, numerical work has been undertaken to study the Lagrangian transport due to breaking induced flow (Deike, Pizzo & Melville 2017). The authors performed a direct numerical simulation of a breaking deep-water wave packet by using a dispersive focusing technique (Rapp & Melville 1990). Particles are tracked during the breaking process and two of these paths are shown in figure 1. Figure 1(*a*) shows a particle that does not surf the breaking wave and has a relatively small horizontal displacement of approximately 0.3 m. Figure 1(*b*) shows a particle, which is initially close to the particle in figure 1(*a*), which surfs the breaking wave and is transported around 2.2 m, which is more than seven times greater than the horizontal displacement in figure 1(*a*). These images motivated this research.

To this end the John equation, which describes the motion of particles on a zero-stress free surface, is considered. Recently, the structure of these equations has been closely examined (Fedele, Chandre & Farazmand 2016), following the development of these equations in three dimensions (Sclavounos 2005). A generalization of this equation has been used to examine the geometry of the surface of breaking waves by Longuet-Higgins (1980, 1982).

In this study, an asymptotic analysis of the behaviour of a perturbed particle obeying the John equation is undertaken. This is found to elucidate a mechanism that is present for particles travelling near the phase velocity of the underlying wave. The analysis yields a criterion for a particle to surf an underlying wave based on the geometry of the free surface and the kinematics of the particle. A generalization of this result is then provided and both results are examined theoretically and numerically.

The outline of this manuscript is as follows. In §2, the equation of John and a criterion for particles to surf an underlying wave are presented. In §3 a breaking deep-water wave is considered and the results are discussed. Finally, in §4 implications of this work are considered.

## 2. Criterion for surfing particles

The equation of John (1953) is presented. Instead of following the original derivation of John, who used the language of complex variables, the work of
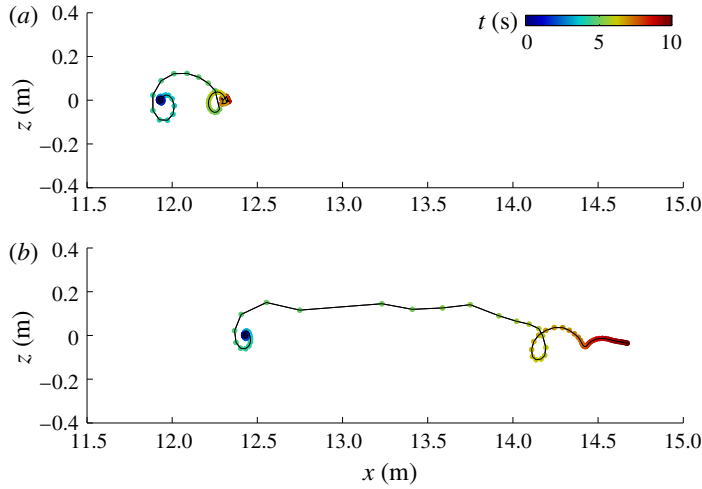
FIGURE 1. (Colour online) Particle displacements for a breaking deep-water wave packet, generated by a direct numerical simulation from Deike *et al.* (2017, see Deike, Popinet & Melville 2015; Pizzo *et al.* 2016 for further discussion of the numerical methods). The linear prediction of the maximum slope at breaking (Drazen, Melville & Lenain 2008) is 0.4, while the central frequency of the packet is 0.88 Hz corresponding to a central wavelength of approximately 2.02 m. The particle trajectory is drawn by the black line, while the time evolution of the particle is indicated by the colour. Dispersive focusing is used to localize energy in space and time (Rapp & Melville 1990) leading to breaking that occurs around $t = 2$ s. Two different particles are shown. In (*a*), the particle does not catch the wave and its displacement is relatively small, approximately 0.3 m. In (*b*), the particle surfs the wave and is displaced a relatively large distance of about 2.2 m, more than seven times further than the non-breaking case.

Sclavounos (2005, see also Fedele *et al.* 2016) is reproduced for completeness (in two spatial dimensions). A criterion for particles to surf an underlying permanent progressive wave is derived. This criterion is then generalized and discussed.

### 2.1. *The John equation*

Recall, for a zero-stress surface the free surface is a line of constant pressure. Furthermore, curves for which $\zeta - \eta$ takes a constant value, where $\eta$ represents the free surface and $\zeta$ is the vertical position of a particle, are level curves. Hence, $\nabla(\zeta - \eta)$ is normal to this level curve. Next, as the pressure gradients must be normal to the surface (the pressure is by definition the isotropic component of the stress), the following relationship holds:

$$\nabla(\zeta - \eta) \times \nabla p = \mathbf{0}; \quad \zeta = \eta. \tag{2.1}$$

The Euler equations in two spatial dimensions are

$$\frac{\mathrm{d}^2 \boldsymbol{\xi}}{\mathrm{d}t^2} = -\frac{1}{\rho} \nabla p + \boldsymbol{g}, \tag{2.2}$$

with $\boldsymbol{\xi} = (\xi(t), \zeta(t))$ the horizontal and vertical positions of the particles, respectively, $\rho$ the density of water, $p$ the pressure and $\boldsymbol{g} = (0, -g)$ the acceleration due to gravity.

Solving for the pressure and substituting this into (2.1) implies

$$\dddot{\xi} + \eta_x(g + \ddot{\zeta}) = 0, \tag{2.3}$$

with dots representing (total) derivatives with respect to time. Next, recall the kinematic boundary condition at the free surface is

$$\dot{\zeta} = \eta_t + \eta_x\dot{\xi}. \tag{2.4}$$

Note, $\dot{\eta} = \eta_t + \eta_x\dot{\xi}$ so that

$$\ddot{\zeta} = \eta_{tt} + \eta_x\ddot{\xi} + 2\eta_{xt}\dot{\xi} + \eta_{xx}\dot{\xi}^2. \tag{2.5}$$

Therefore, equation (2.3) becomes

$$\ddot{\xi} + \left\{ 2\left(\frac{\eta_x\eta_{xt}}{1+\eta_x^2}\right)\dot{\xi} + \left(\frac{\eta_x\eta_{xx}}{1+\eta_x^2}\right)\dot{\xi}^2 + \frac{(\eta_{tt}+g)\eta_x}{1+\eta_x^2} \right\}\Bigg|_{x=\xi} = 0, \tag{2.6}$$

which is the equation found by John (1953). This takes the form of a Ricatti-type equation, with a corresponding variational structure (Sclavounos 2005, see also Fedele *et al.* 2016).

## 2.2. *Surfing criterion for permanent progressive waves*

A criterion for particles to surf an underlying permanent progressive wave is now derived. That is, $\eta(x, t) = \eta(x - ct)$ for some constant phase velocity $c$. Note, permanent progressive waves exist in deep water (e.g. Stokes waves) and shallow water (e.g. soliton and cnoidal solutions to the Korteweg–de Vries equation). This assumption is relaxed in § 2.3, and examined numerically in § 3.

Under the above assumption, the governing equation may be rewritten as

$$\ddot{\xi} + \{F(x-ct)\dot{\xi} + G(x-ct)\dot{\xi}^2 + H(x-ct)\}|_{x=\xi} = 0, \tag{2.7}$$

with $F, G, H$ corresponding to the relevant coefficients in (2.6). Up until this point, the equation still holds exactly for zero-stress free-surface permanent progressive waves under the action of gravity.

The horizontal velocity is decomposed, so that

$$\dot{\xi} = U_0 + u, \tag{2.8}$$

where $U_0$ is the initial velocity of the particle, a constant, and $u = u(t)$ is a perturbation from this value. The particle location $\xi$ can be found by integrating equation (2.8), i.e.

$$\xi = x_0 + U_0 t + \int u \, dt. \tag{2.9}$$

Formally, we take $u \sim O(\epsilon)$ for a small parameter $\epsilon \equiv |u/U_0|$ while $\dot{u} \sim O(1)$, the later assumption being a restriction on the time scale over which this analysis is applicable.

Then, the governing equation to lowest order in $\epsilon$, namely $O(\epsilon^0)$, is

$$\dot{u} - 2U_0 cF(x_0 + \delta t) + U_0^2 G(x_0 + \delta t) + H(x_0 + \delta t) = 0, \tag{2.10}$$

where

$$\delta \equiv U_0 - c, \tag{2.11}$$

which is a measure of how close the initial velocity of the particle is to the phase velocity of the underlying wave.

Substituting in the form of $G$ and $H$ from (2.6) gives

$$\dot{u} + \delta^2 (\log(1 + \eta'^2))' + g\frac{\eta'}{1 + \eta'^2} = 0, \tag{2.12}$$

with primes representing differentiation with respect to $x_0$. Integrating equation (2.12) from 0 to a time $t$ yields

$$\begin{aligned} u = {} & -\delta\{\log(1 + \eta'(x_0 + \delta t)^2) - \log(1 + \eta'(x_0)^2)\} \\ & - g\left\{\frac{N(x_0 + \delta t) - N(x_0)}{\delta}\right\}, \end{aligned} \tag{2.13}$$

where $N$ is the anti-derivative of $\eta'/(1 + \eta'^2)$.

In the limit that the particle speed $U_0$ approaches the phase velocity of the underlying wave, equation (2.13) becomes (using the fundamental theorem of calculus and the definition of the derivative)

$$\lim_{\delta \to 0} u = -g\frac{\eta'}{1 + \eta'^2}t. \tag{2.14}$$

Equation (2.14) provides a criterion for particles to surf the underlying wave. Particles speed up in regions where the right-hand side of (2.14) is positive, so that it is of interest to define the function

$$\mathcal{A} = -g\frac{\eta'}{1 + \eta'^2}. \tag{2.15}$$

The term $-\eta'$ is positive on the forward face of a focusing wave, where the slope is negative, while the denominator is positive definite. This horizontal acceleration (orthogonal to gravity) then acts as a reduced gravity $\mathcal{A}$, which is solely a function of the free-surface geometry and in particular takes on a maximum value when $\eta' = 1$ and hence is bounded by $\pm g/2$.

### 2.3. *Generalized surfing criterion*

The criterion presented in the previous section elucidates the nature of the interaction between the particle and underlying waves. This analysis is valid for small $\epsilon$.

Professor Francesco Fedele (personal communication) has kindly provided a simple argument for the maximum acceleration experienced by particles. This result does not use perturbative analysis nor does it assume the underlying wave is of permanent progressive form.

Following Fedele (2014), consider the collection of curves along the free surface with fixed slope $\alpha_0$. That is, from Longuet-Higgins (1957, equation (2.5.18)), let $x$ and $x + \mathrm{d}x$ be the location of the prescribed slope at times $t$ and $t + \mathrm{d}t$, then

$$\mathrm{d}\eta_x = 0 = \eta_{xt}\,\mathrm{d}t + \eta_{xx}\,\mathrm{d}x = 0, \tag{2.16}$$

so that the speed of propagation of this fixed slope, defined as $c = \mathrm{d}x/\mathrm{d}t$, is given by

$$c = -\frac{\eta_{xt}}{\eta_{xx}}, \tag{2.17}$$

where $c = c(t; \alpha_0)$ is the speed of propagation of the free surface with fixed slope $\alpha_0$. For example, taking $\alpha_0 = 0$ restricts us to following the path of crests or troughs of the wave.

Equation (2.6) can be rewritten as

$$A + \left\{ (U^2 - 2Uc) \left( \frac{\eta_x \eta_{xx}}{1 + \eta_x^2} \right) + \frac{(\eta_{tt} + g)\eta_x}{1 + \eta_x^2} \right\} \bigg|_{x=\xi_P, \eta_x = \alpha_0} = 0, \tag{2.18}$$

where $\xi_P$ is a point on the free surface where the slope is given by $\alpha_0$ and $U = \dot{\xi}_P$ while $A = \ddot{\xi}_P$. Next, the extremum of $A$ is found by varying over all possible slopes, or equivalently over each particle velocity $U$. That is,

$$\frac{\partial A}{\partial U} = 0 \implies U = c, \tag{2.19}$$

which returns the condition found in §2.2. The maximum acceleration, $A(U = c) \equiv A_m$, is then

$$A_m = c^2 \left( \frac{\eta_x \eta_{xx}}{1 + \eta_x^2} \right) - \frac{(\eta_{tt} + g)\eta_x}{1 + \eta_x^2}, \tag{2.20}$$

which is a generalized version of the acceleration given by $\mathcal{A}$.

Note, under the assumption that $\eta = \eta(x - ct)$,

$$A_m = c^2 \left( \frac{\eta' \eta''}{1 + \eta'^2} \right) - \frac{(c^2 \eta'' + g)\eta'}{1 + \eta'^2} = -g \frac{\eta'}{1 + \eta'^2} \equiv \mathcal{A}, \tag{2.21}$$

in agreement with (2.15).

## 3. Numerical example: deep-water perturbed Stokes wave

In order to characterize the behaviour of the acceleration found in the previous section, a perturbed deep-water Stokes wave is examined. This is facilitated through numerical integration of the fully nonlinear potential flow equations (see, for instance, §3.1 of Phillips 1977). A perturbed deep-water Stokes wave (Longuet-Higgins 1978a; Tanaka 1983), with $c = 1.0922$ and $ak = 0.4296$, for $a$ the wave amplitude and $k$ the wavenumber as defined in Longuet-Higgins (1975), is considered. Here, $g = 1$ and the wavelength of the unperturbed Stokes wave is taken to be $2\pi$. The normal mode eigenvalue, and eigenfunction scaling constant, are provided in appendix A.

The evolution of the free surface, in a reference frame moving at the phase velocity of the unperturbed Stokes wave, is shown in figure 2. The leading face of the wave steepens, eventually forming a jet on the forward face of the wave, as shown in the inset of the figure.

Note, I have been representing the free surface as a graph $\eta(x, t)$. However, there is no difficulty in extending this analysis to multivalued free surfaces, parameterized by $(X(s), Y(s))$ a function of the parameter $s \in (0, 2\pi)$.

The particle kinematics are shown in figure 3 which shows the evolution of the velocity, $\dot{\xi}$, and acceleration $\ddot{\xi}$ at various times approaching breaking. The particle
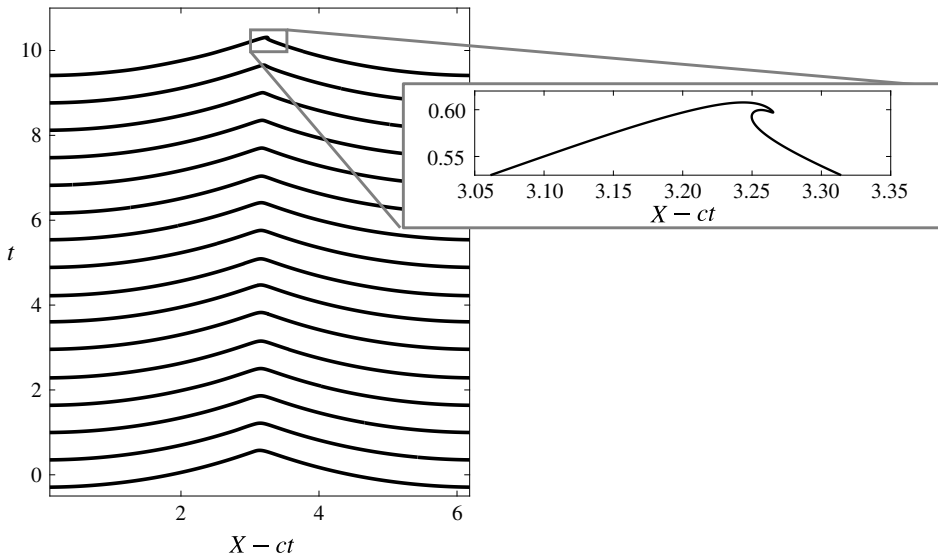
FIGURE 2. The evolution of the free surface of a perturbed deep-water Stokes wave in a frame moving at the phase velocity of the unperturbed Stokes wave, $c$. The forward face of the wave steepens, leading to a jet forming on the forward face of the crest, which is shown in more detail in the inset. Here $c = 1.0922$ and $ak = 0.4296$ and the eigenvalue of the normal mode has value $0.0575$. Refer to text for full details.

velocities approach $c$ in the region where the wave face becomes vertical, with strong horizontal velocities in the jet of the breaking wave (Vinje & Brevig 1981). The initial wave has maximum horizontal fluid velocity that is $0.79c$. As the wave focuses the speed of the particles at the crest increase reaching values exceeding $1.2c$, with an asymmetry forming on the forward face. The accelerations, $\ddot{\xi}$, are initially weak (with an initial maximum value around $0.43g$) and become large (nearly $4g$) in the breaking region as is shown in more detail in figure 5.

The theoretical predictions of the accelerations, $\mathcal{A}$ (red line) and $A_m$ (black line), are shown in figure 4($a$,$b$). Figure 4($a$) shows the evolution of the maximum of $\mathcal{A}$ and $A_m$. Both theories predict a maximum acceleration near the crest of the breaking wave. Figure 4($b$) shows the functional dependence of the accelerations in space. These accelerations become localized as the wave steepens and starts to overturn. Furthermore, in regions where the wave starts to rapidly change its geometry, large accelerations are found and $\mathcal{A}$ is no longer a good approximation and $A_m$ must be employed.

The acceleration in the breaking region is shown in figure 5. The numerical values of the accelerations at two times during the overturning event are shown in ($a$,$c$). Particles travelling within 10 % of the phase velocity of the unperturbed Stokes wave $c$ are highlighted by the gold curves in figures 5($a$) and ($c$), while the corresponding region along the parameter $s$ are shown in ($b$) and ($d$), respectively. These correspond to the regions of maximum acceleration, in accordance with the theoretical results. The theoretical prediction $A_m$ is shown in red, with the numerical velocities shown again by the grey arrows. There is excellent agreement between the theoretical predictions and the numerical results for this example.
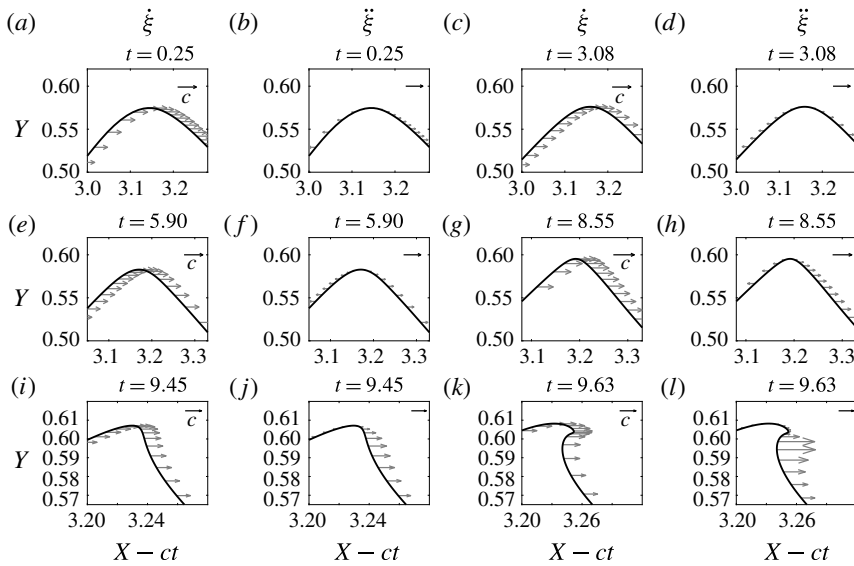
FIGURE 3. Surface particle kinematics for an overturning perturbed deep-water Stokes wave. The horizontal particle velocities $\dot{\xi}$ and accelerations $\ddot{\xi}$ are shown along the free surface at various times as the wave approaches breaking. The maximum velocity of the particles is on the forward face of the crest, and increases during the focusing and breaking event. The arrow in the upper right corner of the acceleration plots has magnitude $g$. There are large accelerations (nearly $4g$ at time $t = 9.63$) just below the crest of the wave on the forward face.

The accelerations become large in this region, reaching values of nearly $4g$. Furthermore, these accelerations become increasing localized to this region underneath the lip of the breaking wave.

## 4. Conclusion

A criterion to surf an underlying wave is derived. This was found by employing the equation of John for a zero-stress free surface under the action of gravity. The optimal location for surfing to occur, for a deep-water perturbed Stokes wave approaching breaking, was established for particles travelling near the phase velocity of the underlying wave and occurs below the crest on the forward face of the wave. Although a deep-water perturbed Stokes wave was considered, this behaviour (sometimes referred to as a crest instability (Longuet-Higgins & Dommermuth 1997)), is characteristic of breaking induced by a variety of methods in both shallow and deep water.

Two approaches were taken. In the first an asymptotic analysis was performed for permanent progressive waves. A generalized criterion was then presented. Both predict that maximum accelerations occur near the crest of the forward face of the wave in a localized region. The asymptotic model breaks down when the free-surface geometry is rapidly varying, and the full description, $A_m$, is needed. This predicts a localized 'sweet spot' to optimally surf a wave.

The phenomenon described in this paper is analogous to Landau damping in plasmas (Landau 1946; Dawson 1961; Mouhot & Villani 2010). Landau damping
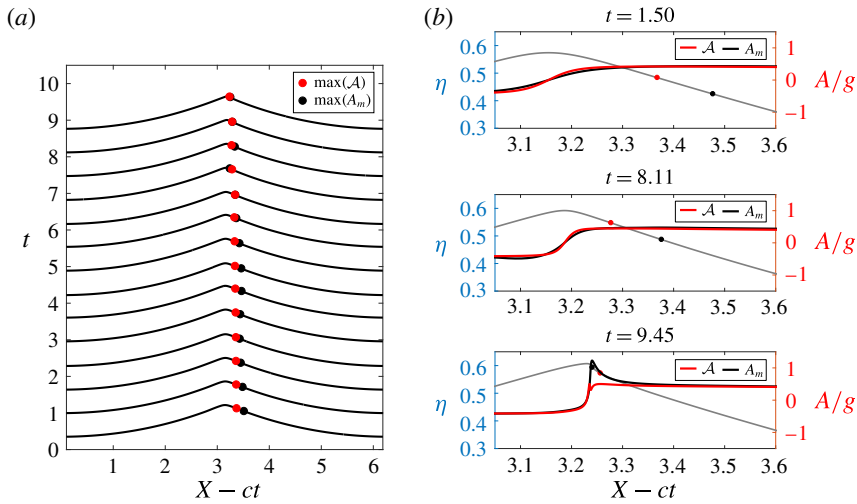
FIGURE 4. (Colour online) (*a*) The locations of the maximum values of the acceleration predicted by the theoretical arguments in §2 along the free surface displacement $\eta$, shown in grey. Both predictions show that the maximum acceleration, that is the surfing sweet spot for the wave, occurs near the crest of the wave on the forward face. (*b*) A comparison of $\mathcal{A}$ (shown in red) and $A_m$ (shown in black) as the wave focuses. Note the scales of the free surface and the accelerations are not the same. The circles show the maximum values of the accelerations. As the packet focuses, both predictions become localized at the crest of the breaking wave. However, $\mathcal{A}$ cannot describe the large accelerations that occur during the formation of the overturning jet. In this region $A_m$ must be employed.

occurs when charged particles encounter an electric field. Particles travelling near the phase velocity of the electric field lose or gain energy based on the initial phase of the electric field and the charged particle. In a qualitative sense then, some charged particles surf the electric field, removing energy from it. This description partially motivated the present study.

The analysis performed in this paper is important for understanding the transfer of energy from the wave field to the water column by wave breaking (Drazen *et al.* 2008; Romero, Melville & Kleiss 2012; Pizzo *et al.* 2016). Here it was found that the perturbed particles increase in speed due to the work done on them by the underlying wave. To adequately quantify the bulk scale behaviour of a collection of particles in a breaking wave, a statistical description of these effects would be necessary. This study might also be of use in better understanding optimal ways for a surfer to surf a wave (Dally 2001). Furthermore, it would be of interest to consider the implications of this study for the capillary rollers found in Longuet-Higgins (1992), with potential implications for a better understanding of the onset of wave breaking (Perlin, Choi & Tian 2013).

Finally, detailed knowledge of the kinematics of particles on the free surface during breaking is currently an active area of research (Deike *et al.* 2017). Laboratory and field analysis of the kinematics and geometry of shallow and deep-water breaking waves is warranted to further corroborate the ideas presented in this paper.
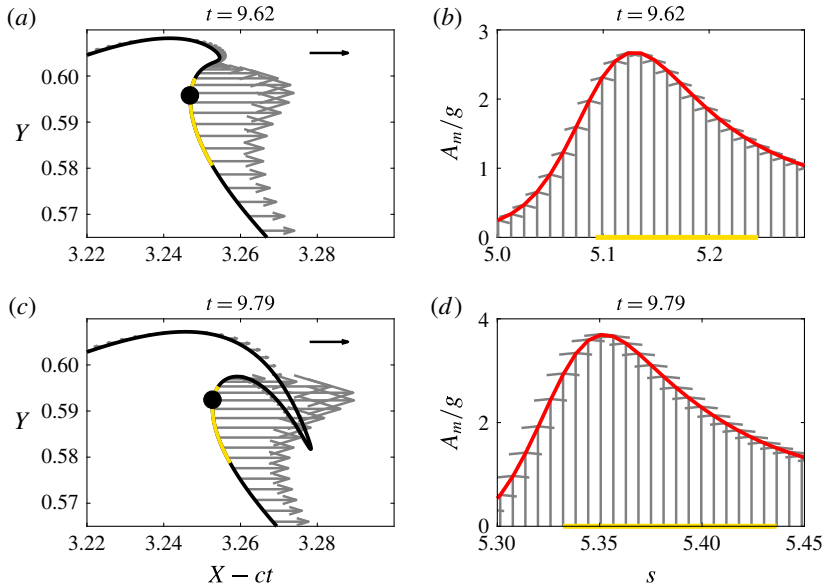
FIGURE 5. (Colour online) Accelerations during the breaking event according to numerically computed values (grey arrows) and theoretical predictions, shown on the right in red. The gold line represents particles travelling at speeds within 10% of the phase velocity $c$, the maximum acceleration is indicated by the black circle and the black arrow in the upper right corner has magnitude $g$. Plots (*b*) and (*d*) show the acceleration along a parameter $s$, with the gold line in (*b*) and (*d*) highlighting the domain of interest corresponding to the gold line in (*a*) and (*c*), respectively. There is good agreement between the theory presented in §2.3 and the numerical values. The large accelerations become spatially localized during the overturning event.

## Acknowledgements

## Appendix A. The Lagrangian of Balk (1996) and the numerical integration of the governing equations

The Lagrangian formulation of the potential flow deep-water surface wave equations, due to Balk (1996) is employed in §3 to find the eigenvalues and eigenvectors of steep Stokes waves (as well as the Stokes coefficients themselves). This formulation has been developed in Pizzo (2015), and a manuscript further analysing these equations is in preparation (Pizzo & Melville 2017). The full details of the model are outside of the scope of the present discussion; however, the basic formulation is presented for completeness.

The dependent variables of the system are $\{Y_{\pm 1}, Y_{\pm 2}, \ldots, Y_{\pm M}\}$ where $M$ is the resolution of the system, and each variable $Y_j$ is a function of time. These variables are related to the parametric description of the surface $(X, Y)$. In particular, $X + \mathrm{i}Y = x + \sum_{k=-M}^{M}(X_k + \mathrm{i}Y_k)\mathrm{e}^{-\mathrm{i}ks}$, where $X_k = \mathrm{i}\sigma_k Y_k$ with $\sigma_k = (-1, 0, 1)$ for $k < 0, k = 0, k > 0$

respectively and $s \in (0, 2\pi)$. The Lagrangian of the system (where recall $g = 1$ and the wavelength is taken to be $2\pi$) may be written as (Balk 1996)

$$L = \frac{1}{2} \sum_{k=-M}^{M} |k| B_k B_{-k} - \frac{1}{2} \sum_{k=-M}^{M} Y_{-k} Y_k - \frac{1}{2} \sum_{k+j+l=0} |l| Y_k Y_j Y_l, \qquad (A\,1)$$

where

$$B_k = \frac{i}{k} \left( -\dot{Y}_k + \sum_{j+l=k} \dot{Y}_j Y_l l(\sigma_j - \sigma_l) \right), \qquad (A\,2)$$

and mass conservation is ensured by setting $Y_0 = -\sum_{k=-M}^{M} |k| Y_k Y_{-k}$.

The equations of motion are found by varying $L$ with respect to $Y_k$ and take the form of a large set of coupled nonlinear ordinary differential equations that are low-order polynomials in the dependent variables. Note, Balk (1996) pointed out that the algebraic set of equations describing Stokes waves takes the natural (quadratic) form (found in a different way by Longuet-Higgins 1978*b*) when $Y_k = \alpha_k e^{ikct}$ for $\alpha_k$ the (constant) Stokes coefficients. The initial conditions were generated by solving this quadratic set of equations for $\alpha_k$ by employing a Newton–Raphson method (Longuet-Higgins 1985). The linear stability analysis was performed by letting $Y_k = (\alpha_k + \Delta A_k(t)) e^{ikct}$ and finding the Lagrangian to $O(\Delta^2)$. This will be discussed in detail in Pizzo & Melville (2017).

The time integration of these equations is efficient unless there are regions of high curvature (Meiron, Orszag & Israeli 1981; Baker & Xie 2011), at which point the spectral coefficients converge slowly and $M$ becomes unreasonably large. Therefore, the time evolution of the system is solved by employing the model of Dold (1992), which has the advantage that points cluster in regions of high curvature, making it extremely efficient. A total of 2048 points were used, with the arc length between points chosen based on the initial particle speed, following Tanaka *et al.* (1987). The scheme of Dold has been verified repeatedly in the literature (see, for example, Dold & Peregrine 1986; Tanaka *et al.* 1987; Dold 1992) and here its accuracy was tested in several ways. First, the Stokes wave considered in this study was propagated, unperturbed, and its stability over two wave periods was observed. Furthermore, the energy was conserved to one part in $O(10^5)$. Next, the equations of Balk were integrated numerically and compared with the results from the scheme of Dold, and accuracy was corroborated leading up to the breaking event. Finally, multiple resolutions were chosen to ensure the scheme converged.

For the example considered in §3, $\lambda \approx 0.0575$ and as the eigenfunction is not unique (it is scale invariant) we take $\Delta = 0.1$. These values are found through the scheme outlined above, and are in agreement with existing studies (Tanaka 1983; Longuet-Higgins & Dommermuth 1997).

## REFERENCES

BAKER, G. R. & XIE, C. 2011 Singularities in the complex physical plane for deep water waves. *J. Fluid Mech.* **685**, 83–116.

BALK, A. M. 1996 A Lagrangian for water waves. *Phys. Fluids* **8** (2), 416–420.

BATTJES, J. A. 1988 Surf-zone dynamics. *Annu. Rev. Fluid Mech.* **20** (1), 257–291.

BRESNAHAN, P. J., WIRTH, T., MARTZ, T. R., ANDERSSON, A. J., CYRONAK, T., DANGELO, S., PENNISE, J., MELVILLE, W. K., LENAIN, L. & STATOM, N. 2016 A sensor package for mapping ph and oxygen from mobile platforms. *Meth. Oceanogr.* **17**, 1–13.

CLARK, D. B., FEDDERSEN, F. & GUZA, R. T. 2010 Cross-shore surfzone tracer dispersion in an alongshore current. *J. Geophys. Res.* **115**, C10.

CRAIK, A. D. & LEIBOVICH, S. 1976 A rational model for Langmuir circulations. *J. Fluid Mech.* **73** (03), 401–426.

DALLY, W. R. 2001 The maximum speed of surfers. *J. Coast. Res.* Special issue 29, 33–40.

DAWSON, J. 1961 On Landau damping. *Phys. Fluids* **4** (7), 869–874.

DEIKE, L., PIZZO, N. E. & MELVILLE, W. K. 2017 Lagrangian transport by breaking surface waves. *J. Fluid Mech.* (submitted).

DEIKE, L., POPINET, S. & MELVILLE, W. K. 2015 Capillary effects on wave breaking. *J. Fluid Mech.* **769**, 541–569.

DOLD, J. W. 1992 An efficient surface-integral algorithm applied to unsteady gravity waves. *J. Comput. Phys.* **103** (1), 90–115.

DOLD, J. W. & PEREGRINE, D. H. 1986 Water-wave modulation. *Coast. Engng Proc.* **1** (20), 163–175.

DRAZEN, D. A., MELVILLE, W. K. & LENAIN, L. 2008 Inertial scaling of dissipation in unsteady breaking waves. *J. Fluid Mech.* **611**, 307–332.

FEDDERSEN, F. 2007 Breaking wave induced cross-shore tracer dispersion in the surf zone: model results and scalings. *J. Geophys. Res.* **112**, C9.

FEDDERSEN, F., OLABARRIETA, M., GUZA, R. T., WINTERS, D., RAUBENHEIMER, B. & ELGAR, S. 2016 Observations and modeling of a tidal inlet dye tracer plume. *J. Geophys. Res* **121**, 7819–7844.

FEDELE, F. 2014 Geometric phases of water waves. *Europhys. Lett.* **107** (6), 69001.

FEDELE, F., CHANDRE, C. & FARAZMAND, M. 2016 Kinematics of fluid particles on the sea surface. Part 1. Hamiltonian theory. *J. Fluid Mech.* **801**, 260–288.

INMAN, D. L., TAIT, R. J. & NORDSTROM, C. E. 1971 Mixing in the surf zone. *J. Geophys. Res.* **76** (15), 3493–3514.

JOHN, F. 1953 Two-dimensional potential flows with a free boundary. *Commun. Pure Appl. Maths* **6**, 497–503.

LANDAU, L. D. 1946 On the vibrations of the electronic plasma. *Zh. Eksp. Teor. Fiz.* **10**, 25–34.

LEIBOVICH, S. 1983 The form and dynamics of Langmuir circulations. *Annu. Rev. Fluid Mech.* **15** (1), 391–427.

LONGUET-HIGGINS, M. S. 1957 The statistical analysis of a random, moving surface. *Phil. Trans. R. Soc. Lond.* A **249** (966), 321–387.

LONGUET-HIGGINS, M. S. 1975 Integral properties of periodic gravity waves of finite amplitude. *Proc. R. Soc. Lond.* A **342**, 157–174.

LONGUET-HIGGINS, M. S. 1978a The instabilities of gravity waves of finite amplitude in deep water. I. Superharmonics. *Proc. R. Soc. Lond.* A **360** (1703), 471–488.

LONGUET-HIGGINS, M. S. 1978b Some new relations between Stokes's coefficients in the theory of gravity waves. *IMA J. Appl. Maths* **22** (3), 261–273.

LONGUET-HIGGINS, M. S. 1980 A technique for time-dependent free-surface flows. *Proc. R. Soc. Lond.* A **371** (1747), 441–451.

LONGUET-HIGGINS, M. S. 1982 Parametric solutions for breaking waves. *J. Fluid Mech.* **121**, 403–424.

LONGUET-HIGGINS, M. S. 1985 Bifurcation in gravity waves. *J. Fluid Mech.* **151**, 457–475.

LONGUET-HIGGINS, M. S. 1992 Capillary rollers and bores. *J. Fluid Mech.* **240**, 659–679.

LONGUET-HIGGINS, M. S. & DOMMERMUTH, D. G. 1997 Crest instabilities of gravity waves. Part 3. Nonlinear development and breaking. *J. Fluid Mech.* **336**, 33–50.

LONGUET-HIGGINS, M. S. & STEWART, R. W. 1964 Radiation stresses in water waves; a physical discussion, with applications. *Deep-Sea Res. Oceanogr. Abstracts* **11** (4), 529–562.

MCWILLIAMS, J. C. & RESTREPO, J. M. 1999 The wave-driven ocean circulation. *J. Phys. Oceanogr.* **29** (10), 2523–2540.

MCWILLIAMS, J. C., RESTREPO, J. M. & LANE, E. M. 2004 An asymptotic theory for the interaction of waves and currents in coastal waters. *J. Fluid Mech.* **511**, 135–178.

MEIRON, D. I., ORSZAG, S. A. & ISRAELI, M. 1981 Applications of numerical conformal mapping. *J. Comput. Phys.* **40** (2), 345–360.

MELVILLE, W. K., VERON, F. & WHITE, C. J. 2002 The velocity field under breaking waves: coherent structure and turbulence. *J. Fluid Mech.* **454**, 203–233.

MOUHOT, C. & VILLANI, C. 2010 Landau damping. *J. Math. Phys.* **51** (1), 015204.

PEREGRINE, D. H. 1983 Breaking waves on beaches. *Annu. Rev. Fluid Mech.* **15** (1), 149–178.

PERLIN, M., CHOI, W. & TIAN, Z. 2013 Breaking waves in deep and intermediate waters. *Annu. Rev. Fluid Mech.* **45**, 115–145.

PHILLIPS, O. M. 1977 *The Dynamics of the Upper Ocean*. Cambridge University Press.

PIZZO, N. E. 2015 Properties of nonlinear and breaking deep-water surface waves. Doctoral thesis. University of California, San Diego.

PIZZO, N. E. & MELVILLE, W. K. 2013 Vortex generation by deep-water breaking waves. *J. Fluid Mech.* **734**, 198–218.

PIZZO, N. E. & MELVILLE, W. K. 2017 A Lagrangian for water waves with application to the stability of stokes waves. (In preparation).

PIZZO, N. E., MELVILLE, W. K. & DEIKE, L. 2016 Current generation by deep-water wave breaking. *J. Fluid Mech.* **803**, 292–312.

RAPP, R. J. & MELVILLE, W. K. 1990 Laboratory measurements of deep-water breaking waves. *Phil. Trans. R. Soc. Lond.* A **331**, 735–800.

ROMERO, L., MELVILLE, W. K. & KLEISS, J. M. 2012 Spectral energy dissipation due to surface wave breaking. *J. Phys. Oceanogr.* **42** (9), 1421–1444.

SCLAVOUNOS, P. D. 2005 Nonlinear particle kinematics of ocean waves. *J. Fluid Mech.* **540**, 133–142.

SINNETT, G. & FEDDERSEN, F. 2014 The surf zone heat budget: the effect of wave heating. *Geophys. Res. Lett.* **41** (20), 7217–7226.

SMITH, J. A. 2006 Observed variability of ocean wave Stokes drift, and the Eulerian response to passing groups. *J. Phys. Oceanogr.* **36** (7), 1381–1402.

SULLIVAN, P. P., MCWILLIAMS, J. C. & MELVILLE, W. K. 2004 The oceanic boundary layer driven by wave breaking with stochastic variability. Part 1. Direct numerical simulations. *J. Fluid Mech.* **507**, 143–174.

SULLIVAN, P. P., MCWILLIAMS, J. C. & MELVILLE, W. K. 2007 Surface gravity wave effects in the oceanic boundary layer: large-eddy simulation with vortex force and stochastic breakers. *J. Fluid Mech.* **593**, 405–452.

TANAKA, M. 1983 The stability of steep gravity waves. *J. Phys. Soc. Japan* **52** (9), 3047–3055.

TANAKA, M., DOLD, J. W., LEWY, M. & PEREGRINE, D. H. 1987 Instability and breaking of a solitary wave. *J. Fluid Mech.* **185**, 235–248.

VINJE, T. & BREVIG, P. 1981 Numerical simulation of breaking waves. *Adv. Water Resour.* **4** (2), 77–82.